rf Electrode Sheath Formation near a Concave Electrode

K E Orlov, D A Malik, T V Chernoiziumskaya, and A S Smirnov

Plasma Physics Department, St. Petersburg State Polytechnical University, Polytechnicheskaya 29, St. Petersburg 195251, Russia

(Received 27 August 2003; published 2 February 2004)

In this work we present experimental results concerning electrode sheath and ion flux formation near a concave electrode with the dimension of a cavity comparable to the electrode sheath length. It is shown that the secondary electron emission can play a crucial role in plasma molding over the electrode surface. It is also observed that plasma has a tendency to "self-leakage" in electrode cavities.

DOI: 10.1103/PhysRevLett.92.055001 PACS numbers: 52.40.Hf, 52.40.Kh

The plasma self-organization scenarios can be drastically affected by electrode and/or vessel geometrical configuration. One of the most spectacular examples is the "hollow cathode" discharge with a cathode filled by cavities [1]. The interaction of plasma with nonflat surfaces also awakens interest regarding various practical applications lasting from a coating of curved objects [2] to a design of observation windows and entering sockets for plasma diagnostic purposes. The processes in the plasma-surface layer depend critically on the shape of the meniscus plasma-sheath boundary formed over the surface topography. A variety of sheath formation scenarios can be commonly classified by using relations between the rf electrode sheath length (L taken as a maximal thickness of the electrode space charge sheath over the rf period) and the characteristic dimension of surface structure (d). In the case when the surface topography scale is considerably less than the characteristic sheath scale ($d \ll L$), the quasineutral plasma cannot be sustained inside cavities [3]. The sheath boundary forms a linear structure, which is practically not affected by electrode morphology. In the opposite case ($d \gg L$), the sheath layer retraces the electrode surface and, except for corner regions, can be also considered as a flat one [4]. In this Letter, we present experimental results concerning sheath structure formation in an intermediate case of cavity dimension comparable with electrode sheath length.

Experiments were carried out using a setup drafted in Fig. 1. The discharge, driven at 13.56 MHz frequency, was burned between two parallel plane duralumin electrodes. The upper electrode, 22 cm in diameter, was connected through a blocking capacitor to an rf generator; the lower electrode was connected to the grounded discharge chamber walls. The setup was equipped by standard electrical diagnostics, thus the applied voltage amplitude, self-bias, rf current, and loaded power were controlled during experiments. Ar was used as operating gas with background pressure 4–30 mtorr. The discharge was operating with a loaded power range from 0.5 to 100 W, which corresponded to an rf voltage amplitude range 100–10^3 V and provided the bulk plasma density (8×10^8)–(5×10^9) cm^{-3} [5]. Because of low operating pressures and the difference in the electrode area, the discharge was asymmetric and the voltage drop in the grounded electrode sheath was lower than on the powered electrode. An energy distribution of ions impinging the grounded electrode surface was controlled by means of a multigrid energy analyzer [6,7]. The analyzer was placed in a differentially pumped high vacuum chamber and connected with a discharge region by a 1 mm diameter orifice. Ion energy distribution functions (IEDF) were obtained by differentiation of the retarding characteristics. The overall ion energy spectra resolution was about 3 eV.

Experiments were performed in two regimes: flat and concave electrode surfaces. The first set of experiments was carried out for commonly used capacitive discharge configuration with flat, parallel electrodes [8]. In the second experimental series, the grounded electrode was equipped by a flat duralumin cover plate with a cylindrical cavity (15 mm diameter, 10 mm height). The axis of the cavity was alignment with a 1 mm inlet orifice of the energy analyzer. In this series, the energy analyzer was able to detect ions flowing to the down faceplate of the cavity.

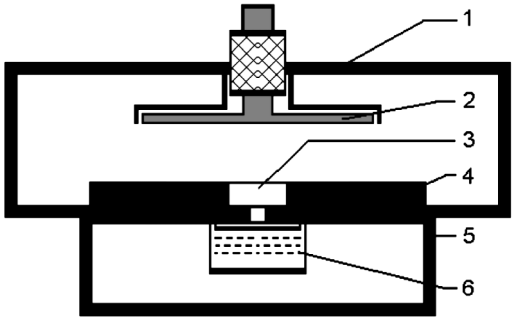

FIG. 1. Schematic drawing of the experimental system; 1, discharge chamber; 2, powered duralumin electrode with ground shield; 3, cavity on the grounded electrode; 4, grounded duralumin electrode; 5, high vacuum chamber; 6, multigrid energy analyzer.

Experimentally observed ion spectra are presented in Fig. 2. For the flat electrode regime, the IEDF always has a clearly pronounced peak at the high-energy part. The IEDF measured at the bottom faceplate of the cavity shows more complicated behavior. In the low power regime, the IEDF, gradually with the power, switches from the single-peaked shape to a two-peaked one. With an increase of the loaded power, the height of the low-energy peak increases while its energy remains approximately constant. The high-energy peak is also observed and its energy increases with loaded power increasing. With a further increase of loaded power, the IEDF transforms back from the two-peaked shape to the single-peaked one with one high-energy peak.

In the low-pressure case considered here, the ionization in the sheath is negligible. Because of nonlocality conditions for the bulk electrons, they do not have enough kinetic energy to produce ionization in the sheath region [9]. The secondary electrons, emitted from the electrode surface, are accelerated towards the plasma body by a momentary value of voltage drop in the sheath [10,11]. It always considerably exceeds the ionization potential, and the secondary electrons are capable of producing ionization. However, their mean-free path with respect to ionization collisions [12] ($\lambda_e^i \sim 15$ cm for the conditions of Fig. 2) exceeds any reasonable sheath length values, and secondary electrons can produce ionization only in the plasma bulk. Consequently, the ions are supplied to the sheath from plasma bulk, and their flux is conserved through the sheath.

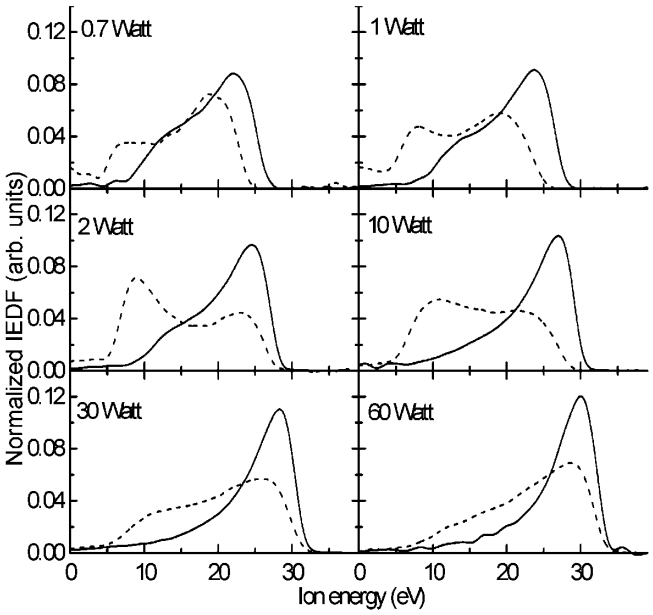

FIG. 2. Energy distribution functions of ions bombarding the flat electrode surface (solid line) and the down faceplate of the cylindrical cavity (dashed lines) at different values of discharge loaded power. Ar, $p = 5$ mtorr.

The ion mean-free path with respect to charge-exchange collisions [12] ($\lambda_i \sim 10$ cm) exceeds the sheath length, and ion spectra is formed by collisionless ion acceleration. So, the ion spectra are close to monochromatic (see full lines in Fig. 2) with energy equal to the averaged potential drop in the sheath $\langle U \rangle$ (for a perfectly collisionless situation [13] $\langle U \rangle = 0.43 U_{\max}$, where $U_{\max}$ is a maximal voltage drop in the sheath during rf period). The distribution slope towards low energies is formed due to nonzero charge-exchange collision probability and can be roughly fitted by an exponential dependence $\sim \exp(-L/\lambda_i)$.

The flat sheath parameters can be easily estimated by using the measured IEDF and well developed collisionless sheath theory [13,14]. The ion flux to the electrode is proportional to the ion density and velocity at the electrode surface $j_i \sim n_i(\langle U \rangle)^{0.5}$. This provides, for the conditions of Fig. 2, the ion density growing with power from 3×10^7 to 2×10^8 cm^{-3}. The sheath length can be related to ion density and sheath voltage as shown in [13]. Obtained from the experimentally observed j_i and $\langle U \rangle$, the sheath length values are presented in Fig. 3. In the regime with the concave electrode, far from the cavity, the sheath should be identical to the sheath at the flat electrode. As the cavity diameter in our experiments is in the same order of magnitude as doubled unperturbed sheath length ($d \sim 2L$), the sheath structure in the cavity region is sufficiently two dimensional [Fig. 4(a)]. It should also be noted that, due to the divergence of ion trajectories, the local sheath length (L^*) in the cavity vicinity is larger than the flat sheath length [4] (L). A stationary quasineutral plasma cannot be sustained inside the cavity until $2L^* > d$.

The observed low-energy IEDF fraction in the concave electrode (Fig. 2) can be explained by a subsidiary ionization in the cavity. The low-energy ions are produced inside the cavity, where the averaged potential is lower,

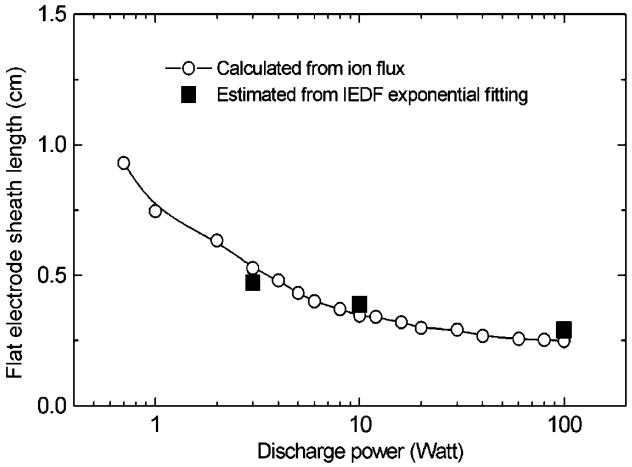

FIG. 3. Flat unperturbed sheath length for the conditions of Fig. 2.

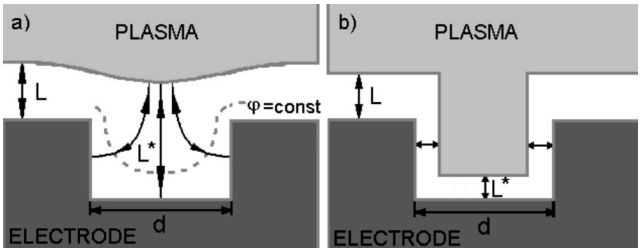

FIG. 4. Illustration of a sheath structure near the cylindrical cavity for different ratios of the cavity diameter (d) and the local sheath length (L^*). Left picture corresponds to the case $2L^* > d$, right to the case $2L^* < d$. Lines with arrows schematically show plasma-space charge boundary oscillations during the rf period.

while the high-energy ions are traveling from the bulk plasma and are accelerated by the total voltage drop in the sheath. The ionization in the sheath can be produced only by secondary electrons. The radial motion of secondary electrons in the cavity is trapped by a potential well. The bouncing between the potential walls leads to an increase of the electron path in the cavity and, as a result, enhances the ionization rate in the cavity region. The existence of a considerable ionization by secondary electrons in the cavity is also confirmed by the fact that the total ion current from the cavity grows with power faster than ion current to the flat part of the electrode. The increase of the power loaded in the discharge leads to the increase of the sheath potential, ion energy, ion flux, and secondary electron emission rate. Simultaneously, the ionization rate and ion density in the cavity grow up. The rise of the ion density in the cavity leads to a local decrease of the sheath length L^*. When the ionization inside the cavity increases, the condition $2L^* < d$ becomes satisfied. Now, the cavity becomes filled up by the stationary quasineutral plasma and a thin electrode sheath is faced parallel to the cavity surface as it is schematically illustrated in Fig. 4(b). This being the case, the ions borne in the cavity are accelerated by the total potential drop in the sheath and the low-energy fraction of IEDF disappears.

This work was supported by NATO SfP Grant No. 974354 and RBRF Grant No. 01-02-16874. The authors wish to thank Professor L. D. Tsendin for helpful discussions.

[1] B. I. Moskalev, in *Hollow Cathode Discharges* (Energoizdat, Moscow, 1969).
[2] H. R. Kaufman and R. S. Robinson, in *Handbook of Plasma Processing Technology*, edited by S. M. Rossnagel, J. J. Cuomo, and W. D. Westwood (Noyes, New Jersey, 1990).
[3] Chang-Koo Kim and D. J. Economou, J. Appl. Phys. **91**, 2594 (2002).
[4] Doosik Kim, D. J. Economou, J. R. Woodworth, P. A. Miller, R. J. Shul, B. P. Aragon, T.W. Hamilton, and C. G. Willison, IEEE Trans. Plasma Sci. **31**, 691 (2003).
[5] A. S. Smirnov and K. E. Orlov, Tech. Phys. Lett. **23**, 26 (1997).
[6] C. Bohm and J. Perrin, Rev. Sci. Instrum. **64**, 31 (1993).
[7] A. S. Smirnov, A. Y. Ustavshchikov, and K. S. Frolov, Zh. Tekh. Fiz. **65**, 38 (1995).
[8] K. Kohler, J. W. Coburn, D. E. Horne, and E. Kay, J. Appl. Phys. **57**, 59 (1985).
[9] L. D. Tsendin, Plasma Sources Sci. Technol. **4**, 200 (1995).
[10] P. W. May, D. F. Klemperer, and D. Field, J. Appl. Phys. **73**, 1634 (1993).
[11] K. E. Orlov and A. S. Smirnov, IEEE Trans. Plasma Sci. **27**, 1348 (1999).
[12] E. W. McDaniel, in *Collision Phenomena in Ionized Gases* (Wiley, New York, 1964).
[13] M. A. Lieberman, IEEE Trans. Plasma Sci. **16**, 638 (1988).
[14] T. Panagopoulos and D. J. Economou, J. Appl. Phys. **85**, 3435 (1999).